BMC Genomics

RESEARCH

Open Access

Comprehensive identification of maize ZmE2F transcription factors and the positive role of *ZmE2F6* in response to drought stress

Yang Cao[1†], Kexin Wang[1†], Fengzhong Lu[1], Qi Li[1], Qingqing Yang[1], Bingliang Liu[2], Hayderbinkhalid Muhammad[3], Yingge Wang[1], Fengling Fu[1], Wanchen Li[1] and Haoqiang Yu[1*]

Abstract

Background The early 2 factor (E2F) family is characterized as a kind of transcription factor that plays an important role in cell division, DNA damage repair, and cell size regulation. However, its stress response has not been well revealed.

Results In this study, ZmE2F members were comprehensively identified in the maize genome, and 21 *ZmE2F* genes were identified, including eight *E2F* subclade members, seven *DEL* subfamily genes, and six DP genes. All ZmE2F proteins possessed the DNA-binding domain (DBD) characterized by conserved motif 1 with the RRIYD sequence. The ZmE2F genes were unevenly distributed on eight maize chromosomes, showed diversity in gene structure, expanded by gene duplication, and contained abundant stress-responsive elements in their promoter regions. Subsequently, the *ZmE2F6* gene was cloned and functionally verified in drought response. The results showed that the ZmE2F6 protein interacted with ZmPP2C26, localized in the nucleus, and responded to drought treatment. The overexpression of *ZmE2F6* enhanced drought tolerance in transgenic *Arabidopsis* with longer root length, higher survival rate, and biomass by upregulating stress-related gene transcription.

Conclusions This study provides novel insights into a greater understanding and functional study of the E2F family in the stress response.

Keywords Maize, E2F, Transcription factor, Expression, Drought stress

Background

Environmental stimuli, including drought, salinity, and high temperature, have frequently occurred in recent decades and led to yield loss of crops in agricultural production. Drought stress is a main misfortune in these abiotic stressors and will be a more severe challenge and threat to agriculture and humanity by 2050 [1]. In adaption to drought, plants activate a series of physiological, morphological, and molecular changes [1–3]. Among them, many transcription factors (TFs) can be dominated by stress to regulate gene expression and coordinate plant antagonism to adverse factors [4–6].

†Yang Cao and Kexin Wang contributed equally to this work.

*Correspondence:
Haoqiang Yu
yhq1801@sicau.edu.cn
[1]Maize Research Institute, Sichuan Agricultural University, Chengdu 611130, China
[2]College of Food and Biological Engineering, Chengdu University, Chengdu 610106, China
[3]National Research Centre of Intercropping, The Islamia University of Bahawalpur, Bahawalpur 63100, Pakistan

The early E2 factor (E2F) family proteins are initially discovered as TFs of the *E2* gene and play key roles in cell proliferation control in adenoviruses [7]. E2Fs can be classified into typical and atypical E2Fs according to protein structure. Typically, E2Fs have only one DNA-binding domain (DBD) and form heterodimeric complexes with dimerization proteins (DPs) to bind the promoters of downstream genes, but atypical E2Fs possess duplicated two DBD [8]. In higher plants, E2Fs are also categorized into three subclades, including E2F, DP, and DEL (DP-E2F-like), due to the difference in the composition of conserved domains [9, 10]. Over the past decade, E2Fs have well been revealed to play significant roles in the cell cycle and DNA damage repair [11–16]. For instance, ectopic expression of *DcE2F1* of *Daucus carota* promotes cell proliferation in *Arabidopsis* seedlings [14]. In *Arabidopsis*, eight E2F members exhibit antagonistic roles in cell proliferation, such as E2Fa/b, which acts as a positive regulator, but E2Fc is a negative regulator [17–19]. E2Fa/b can also activate the DNA damage response and cell cycle progression by differentially regulating the expression of genes [11]. Additionally, AtE2Fa/DPa also inhibits growth, and *AtE2Fa/DPa*-overexpressing plants show an abnormal phenotype owing to ectopic cell division or enhanced DNA endoreduplication [12, 20].

In addition to the crucial role in the cell cycle, few reports show that atypical E2F inhibits the accumulation of salicylic acid to balance growth and defense [21, 22]. Furthermore, AtE2Fa acts downstream of ERECTA kinase, which is involved in cell size and stomatal density [23]. Via expression analysis, it is suggested that *TaE2F-DP* of wheat, *PheE2F/DPs* of Moso bamboo, *E2F/DP* genes of *Medicago truncatula*, and *PvE2F/DPs* of *Phaseolus vulgaris* respond to drought or salt stress, suggesting their potential roles in regulating stress tolerance [9, 24–26]. To date, however, the role of E2F in plant stress tolerance remains obscure.

Maize is a crucial crop worldwide and is widely used as food and livestock feed. During its growth, maize plants show sensitivity to water deficit due to its high water demand, leading to maize yield being greatly affected by drought stress [27–30]. Therefore, it becomes imperative to identify and explore drought tolerance-related genes that can be used to enhance maize resilience through molecular breeding [31–35]. In our previous study, we found that ZmPP2C26 regulated drought tolerance [36] and targeted maize ZmE2F (Zm00001d048412, data not shown), indicating that ZmE2F might be involved in drought response. Hence, in this study, we comprehensively investigated *ZmE2F* genes in the maize genome. Thereafter, phylogenetic relationships, conserved motifs and domains, gene structures and duplication, and protein-protein interaction networks were analyzed. Additionally, the ZmE2F6 (Zm00001d048412) was functionally verified by performing subcellular localization, expression patterns in drought treatment, and ectopic expression in *Arabidopsis* under drought stress. This study will significantly contribute to a better understanding of E2Fs in stress response.

Methods

Identification of *ZmE2Fs* in the maize genome

The genome and amino acid data of maize B73 were downloaded from the MaizeGDB database (https://download.maizegdb.org/Zm-B73-REFERENCE-GRAMENE-4.0/). Meanwhile, the coding sequences and amino acid sequences of 8 AtE2Fs and 9 OsE2Fs of *Arabidopsis* and rice were downloaded from the *Arabidopsis* Information Resource (TAIR) (https://www.arabidopsis.org/) and the Rice Genome Annotation Project (RGAP) database (http://rice.uga.edu/) and were used as queries to perform local BLASTp with an E-value of $1e^{-10}$ in the maize protein database for maize E2F searching, respectively. After removing the redundant sequences manually, the candidate sequences were further analyzed for the presence of the E2F_DP domain (PF02319) by using PFAM (http://pfam.xfam.org/). The candidates possessing the E2F domain were identified as maize ZmE2F members. The secondary structure and physicochemical properties, including molecular weights, isoelectric point (PI), stability coefficient, and grand average of hydropathicity (GRAVY), of ZmE2Fs were analyzed using SOPMA (https://npsa.lyon.inserm.fr/cgi-bin/npsa_automat.pl?page=/NPSA/npsa_sopma.html) and EXPASY (https://www.expasy.org/). The subcellular localization of ZmE2Fs was predicted using cNLS Mapper (https://nls-mapper.iab.keio.ac.jp/cgi-bin/NLS_Mapper_form.cgi).

Conserved motifs, domains, and phylogenetic analysis

To further identify the conserved motifs and domains, the amino acid sequences of ZmE2Fs were analyzed using MEME (http://meme-suite.org/tools/meme) and NCBI-CDD (https://www.ncbi.nlm.nih.gov/cdd), respectively. The motif and domain composition of each ZmE2F was visualized by TBtools [37]. The protein sequences of all ZmE2F, AtE2F, and OsE2F were multiple-aligned using ClustalW with default parameters. The maximum likelihood tree was built with 1000 bootstrap replications by MEGA11 (https://www.megasoftware.net/). Meanwhile, protein-protein interaction (PPI) analysis among ZmE2F members was performed using the STRING tool [38].

Gene structure, promoter, duplication, and synteny analyses

The chromosomal location of each *ZmE2F* gene was obtained from the maizeGDB database. The coding sequences and genomic DNA sequences of every *ZmE2F* were downloaded and used to analyze exon-intron

composition using Gene Structure Display Server 2.0 (GSDS) (http://gsds.gao-lab.org/). The 2000 bp upstream sequence of the transcription start site of each *ZmE2F* gene was retrieved from maizeGDB and used for *cis*-acting element analysis using PlantCARE (https://bioinformatics.psb.ugent.be/webtools/plantcare/html/). Meanwhile, the gene duplication events and the synteny relationship between *ZmE2F*, *AtE2F*, and *OsE2F* gene members were analyzed using MCScanX with default parameters. The chromosomal location, duplications, and synteny relationships of the *ZmE2F*, *AtE2F*, and *OsE2F* genes were visualized using TBtools [37]. The non-synonymous (Ka) and synonymous (Ks) substitution rates per site of the duplicated gene pairs were calculated using TBtools [37]. Then, the divergence time in millions of years (Mya) was also calculated using the following formula: $T=Ks/2\lambda\times10^{-6}$ Mya ($\lambda=6.5\times10^{-9}$ for grasses) [39].

Cloning and subcellular localization of the *ZmE2F6* gene

The specific primers (Table S1) were designed by Primer 5.0, synthesized at Tsingke Biotech (Beijing, China), and used to amplify the sequence of the *ZmE2F6* gene from maize B73 cDNA using Phanta Max Super-Fidelity DNA Polymerase (Vazyme, Nanjing). After amplification, the PCR product was purified by a gel recovery kit subcloned, and inserted into the pMD19-T vector to generate pMD19-T-*ZmE2F6* and verified by sequencing. The sequencing result was aligned with the candidate sequence of the *ZmE2F6* gene using DNAMAN. The open reading frame (ORF) sequence of *ZmE2F6* without stop codon was amplified from the pMD19-T-*ZmE2F6* plasmid using the specific primers designed by CE Design V1.04 (Table S1) with the *Xba* I and *Spe* I recognition sites. The PCR products and pCAMBIA2300-*35 S-eGFP* plasmids were digested using *Xba* I and *Spe* I. Subsequently, they were inserted into the *Xba* I and *Spe* I sites of pCAMBIA2300-*35 S-eGFP* to produce the fusion expression vector *35 S-ZmE2F6-eGFP* using the ClonExpress II One Step Cloning Kit (Vazyme, Nanjing). Each construct was introduced into *Agrobacterium tumefaciens* strain GV3101 and then used for transient expression in the leaves of *Nicotiana benthamiana*. As described by Sun et al. [40], the constructs were infiltrated into the leaves of five-week-old *N. benthamiana*. The GFP fluorescence was observed and imaged using a confocal laser scanning microscope (Zeiss 800). The empty vector *35 S-eGFP* was served as the positive control.

Plant treatment, RNA extraction, and quantitative real-time PCR (qRT–PCR) analysis

The seeds of maize B73 lines were soaked in 10% H_2O_2 for 15 min, rinsed twice using sterile water, soaked in distilled water for 8 h, then wrapped in filter paper and cultured at 28 °C until germination. Subsequently, the seedlings of the same size were transferred to the hydroponic cassette containing hoagland nutrient solution and cultured at 16 h light at 28 °C /8 h dark at 24 °C. Three-leaf-stage seedlings were subjected to 16% PEG-6000 treatment mimicking drought stress, and then shoots containing leaf, stem and leaf sheath, and roots were sampled at 0, 3, 6, 12, and 24 h of treatment, respectively. The total RNA of each sample was extracted using an RNAison plus kit (Takara, Dalian), examined for quality using NanoDrop OneC (ThermoFisher Scientific), treated with DNase to remove DNA contamination, reverse-transcribed into cDNA using a PrimeScript™ RT Regent Kit (Takara, Dalian), and used to perform qRT-PCR. The specific primers of *ZmE2F6* were designed using Primer-BLAST (https://www.ncbi.nlm.nih.gov/tools/primer-blast/index.cgi?LINK_LOC=BlastHome), synthesized at TsingkeBiotech (Beijing, China), and listed in Table S1. The *ZmGAPDH* gene was amplified using specific primers (Table S1) and used as an internal reference. The qRT-PCR was performed in the Bio-Rad CFX96™ Real-Time PCR system using 2 × Universal SYBR Green Fast qPCR Mix (ABclonal, Wuhan). The 20 μL reaction mixture contained 10 μL of 2 × Universal SYBR Green Fast qPCR Mix, 0.4 μL of each forward and reverse primer, 1.0 μL of each cDNA as template, and 8.2 μL of ddH_2O. The reaction protocol was set as a two-step temperature cycle including 95 °C for 3 min, followed by 40 cycles at 95 °C for 5 s and 60 °C for 30 s. The relative expression level of *ZmE2Fs* was calculated and normalized using the $2^{-\Delta\Delta Ct}$ method [41].

Y2H and GST pull-down analysis

The ORF of *ZmE2F6* was amplified using specific primers designed by CE Design V1.04 with the *Nde I* and *EcoR I* recognition sites (Table S1) and inserted into the pGADT7 plasmid to generate AD-*ZmE2F6* as described above. The BD-*ZmPP2C26* plasmid was constructed in our previous study [36]. The AD-*ZmE2F6* and BD-*ZmPP2C26* plasmids were cotransformed into the yeast strain Y2H Gold using a yeast transformation kit (Coolaber, Beijing). Subsequently, yeast cells were cultured on synthetic dropout (SD) medium without Trp and Leu (SD/-Trp/-Leu) at 30℃ for 2 days, and then positive clones were transferred onto SD/-Trp/-Leu/-His/-Ade plates with X-α-gal and cultured at 30℃ for 2 days. Meanwhile, the ORF of *ZmE2F6* was amplified and inserted into the *EcoR I* and *Xho I* sites of pGEX-6P-1 to generate *GST-ZmE2F6* and used for the GST pull-down assay. The *His-ZmPP2C26* plasmids were produced in our previous study. The GST pull-down was performed as described by Lu et al. [36].

Plant transformation, phenotyping, and RNA-seq

The ORF of *ZmE2F6* was amplified without a stop codon and inserted into the *Xba* I and *Nde* I sites of pRI201-*35 S-GUS* to produce *35 S-ZmE2F6-GUS* as described above. The *35 S-ZmE2F6-GUS* construct was transformed into *Agrobacterium tumefaciens* strain GV3101 and then used to transform *Arabidopsis thaliana* (Col-0) by the floral-dip method [42]. According to the method of Sun et al. [40], the positive transformants were screened on 1/2 MS plates with 50 mg/L kanamycin, used for harvesting seeds individually. The homozygous lines without segregation on 1/2 MS plates with 50 mg/L kanamycin were screened and used for PCR detection. Meanwhile, the leaves of homozygous lines were sampled and used to perform GUS staining using the GUS Staining Kit (Coolaber, Beijing).

According to the methods described by Sun et al. [40] with minor modifications, for drought stress, the seeds of homozygous lines and wild type (WT) were surface-sterilized, planted on 1/2 MS plates supplemented with 0 (control), 150, and 250 mM mannitol, vernalized for 2 days in the dark at 4 °C, and vertically cultured in a chamber under 10 h light/14 h dark at 22 °C with 60–70% humidity. At 14 days of treatment, the seedlings were photographed and measured for root length. Moreover, another batch of overexpressed lines and WT were sown in soil and incubated in a greenhouse under the same conditions. After 2 weeks, the seedlings were subjected to withholding water for two weeks, then rewatered for at least 2 days, and monitored for phenotyping. Subsequently, the survival number of each line was counted and used to calculate the survival rate. The leaf of each line was sampled, dried at 80 °C for 3 days, and used for biomass measurement.

Meanwhile, three-week-old seedlings of homozygous lines and WT were sampled and used for RNA sequencing at Sanshubio Company (Jiangsu, China). As described by Sun et al. [40], the total RNA of each sample was extracted, qualified for quality and integrity, and used to construct a sequencing library. Then, library sequencing was conducted using the NovaSeq 6000 system. The sequencing adapters and low-quality reads of raw data were removed to generate clean data, which were mapped to the *Arabidopsis* genome by hisat2 [43] and used for assembling transcripts of every gene using StringTie [44]. The differentially expressed genes (DEGs) were confirmed with a p-value < 0.05 and |FoldChange| > 2 using DESeq2 [45]. The GO analysis of DEGs was performed using KOBAS [46].

Data analysis

All assays were performed with three replicates. The data are shown as the mean values ± standard error (SE). The significance was analyzed by Student's t-test at the $p < 0.05$ or $p < 0.01$ level.

Results

ZmE2F members in maize

To identify the maize *ZmE2F* family, a local BLASTp search against the maize protein database was performed using the amino acid sequences of 8 *AtE2F* and 9 *OsE2F* members as query references [10, 47]. As shown in Table 1, a total of 21 ZmE2F members were identified and designated as *ZmE2F1* to *ZmE2F21*. The CDS length of the ZmE2F genes ranged from 648 (*ZmE2F18*) to 1608 bp (*ZmE2F14*), encoding 215 to 535 amino acids with molecular weight varying from 23.39 to 59.21 kDa. The theoretical isoelectric point (pI) of ZmE2F proteins ranged from 4.71 (ZmE2F11) to 9.41 (ZmE2F13), and the grand average hydropathicity (GRAVY) of all ZmE2F proteins was less than 0 and ranged from −0.062 (ZmE2F1) to -0.603 (ZmE2F5). The instability indices of ZmE2F proteins varied from 31.45 (ZmE2F20) to 62.39 (ZmE2F5), and 19 ZmE2F members contained the highest random coil in their secondary structure, implying that they were unstable hydrophilic proteins. All ZmE2F proteins were predicted to be localized in the nucleus.

Phylogenetic analysis

To investigate the evolutionary relationships of ZmE2Fs and model plants, a total of 38 amino acid sequences, including 21, 8, and 9 E2Fs from maize, *Arabidopsis*, and rice, respectively, were used to construct a phylogenetic tree (Fig. 1). It showed that the ZmE2F proteins could be classified into three subfamilies, including E2F, DP, and DEL clades [9]. Eight members, including ZmE2F2, 4, 5, 11, 14, 16, 17, and 21, were clustered into the E2F subscale with AtE2Fs and OsE2Fs. Seven proteins containing ZmE2F1, 7, 10, 12, 13, 15, and 20 were branched into the DEL subfamily with AtDELs and OsDELs. The other 6 ZmE2Fs (ZmE2F3, 6, 8, 9, 18, and 19) belonged to the DP subclade with AtDP and OsDP members. In addition, ZmE2Fs showed a closer phylogenetic relationship with OsE2Fs than with AtE2Fs, indicating more sequence similarity with OsE2Fs.

Conserved motif and domain

Five conserved motifs were identified in the amino acid sequences of ZmE2Fs using the MEME online program (Fig. 2A). Among them, motif 1 was highly conserved in all ZmE2F members and characterized by the RRIYD sequence that was a DNA-binding motif followed by dimerization residues DNVLE sequence [48]. Conserved domain analysis revealed that all ZmE2F members contained at least one DNA-binding domain (DBD) (Pfam ID PF02319, Table S2). ZmE2F7, 12, and 13 possessed two DBDs (Fig. 2B). In addition, ZmE2F5, 6, 9, 18, and 19 also

Table 1 The physical and chemical properties of ZmE2F family

Gene name	Gene ID	CDS length (bp)	Protein length (aa)	Mass (kDa)	PI	II	GRAVY	Secondary structure (%)			Localization
								Alpha helix	Extended strand	Random coil	
ZmE2F1	Zm00001d032741	1002	333	37.09	5.99	39.96	-0.062	31.23	18.62	43.84	N
ZmE2F2	Zm00001d007384	966	321	34.96	9.01	47.97	-0.441	38.32	13.71	41.12	N
ZmE2F3	Zm00001d033566	852	283	33.07	6.60	50.03	-0.533	30.04	21.55	43.11	N
ZmE2F4	Zm00001d016737	1392	463	50.56	5.05	53.43	-0.566	26.35	10.80	60.69	N
ZmE2F5	Zm00001d004512	1407	468	50.68	5.70	61.97	-0.603	24.36	10.26	62.39	N
ZmE2F6	Zm00001d048412	1233	410	44.39	6.02	51.02	-0.570	30.98	11.22	53.90	N
ZmE2F7	Zm00001d017986	1344	447	49.25	9.18	41.18	-0.561	37.81	6.94	51.90	N
ZmE2F8	Zm00001d016907	852	283	33.23	6.84	51.53	-0.584	33.22	21.20	39.58	N
ZmE2F9	Zm00001d011597	759	252	28.38	9.27	48.17	-0.487	47.62	9.13	38.10	N
ZmE2F10	Zm00001d045365	732	243	27.19	7.64	40.53	-0.227	33.74	20.99	38.27	N
ZmE2F11	Zm00001d023465	1368	455	49.67	4.71	50.12	-0.592	27.91	11.43	57.14	N
ZmE2F12	Zm00001d037274	1308	435	48.10	8.80	50.34	-0.567	37.01	7.82	53.33	N
ZmE2F13	Zm00001d052288	1335	444	48.70	9.41	45.74	-0.523	40.09	8.11	48.87	N
ZmE2F14	Zm00001d038664	1608	535	59.21	8.44	46.46	-0.346	37.57	18.50	35.70	N
ZmE2F15	Zm00001d026355	777	258	28.76	6.06	62.33	-0.555	18.60	15.50	59.69	N
ZmE2F16	Zm00001d050664	1131	376	40.89	5.35	48.64	-0.401	26.06	13.56	58.78	N
ZmE2F17	Zm00001d003755	1104	367	40.73	9.03	43.78	-0.485	29.97	11.44	56.13	N
ZmE2F18	Zm00001d014132	648	215	23.39	6.84	57.36	-0.540	43.72	4.19	48.84	N
ZmE2F19	Zm00001d027709	1161	386	41.49	6.09	50.25	-0.748	30.05	10.62	55.44	N
ZmE2F20	Zm00001d045639	837	278	30.97	8.75	31.45	-0.601	32.73	18.71	44.96	N
ZmE2F21	Zm00001d046856	1602	533	58.57	8.55	44.61	-0.224	32.27	21.95	36.77	N

contained a dimerization domain (DD). The coiled coil (CC)-marked box (MB) domain (CC-MB) was found in ZmE2F4, 11, 16, and 17. Furthermore, all ZmE2F members contained a nuclear localization signal.

ZmE2Fs protein-protein Interaction Prediction

Due to the presence of dimerization residues DNVLE sequence within motif 1 in every ZmE2F and DD or CC-MB in some ZmE2Fs, to explore the potential interactions among ZmE2F members, protein-protein interaction (PPI) analysis was performed. As shown in Fig. 3, ten ZmE2Fs were predicted to interact with each other, which generated 23 PPI combinations. Among them, ZmE2F6, 9, 18 and 19 had the largest number of PPIs (6 interactions), while ZmE2F4, 5, 11, 14, 16, and 17 had 4 PPIs. These results imply that the DNVLE sequence, DD, and CC-MB play crucial roles during ZmE2F dimerization.

Gene structure, duplication, synteny, and *cis* -acting elements

Gene structure analysis revealed that the *ZmE2F* gene family showed diversity in exon and intron composition (Fig. 4A). The number of exons among *ZmE2Fs* ranged from six to fourteen. Except for *ZmE2F18* and *ZmE2F20*, the other 19 *ZmE2Fs* contained 5′ or 3′ terminal untranslated regions. The *ZmE2Fs* were unevenly distributed on eight maize chromosomes, excluding chromosomes 3 and 7. Gene duplication analysis showed that there were eight paralogous pairs of *ZmE2Fs* in the maize genome, including *ZmE2F4* and *ZmE2F17*, *ZmE2F6* and *ZmE2F18*, *ZmE2F6* and *ZmE2F19*, *ZmE2F7* and *ZmE2F12*, *ZmE2F7* and *ZmE2F13*, *ZmE2F11* and *ZmE2F17*, *ZmE2F12* and *ZmE2F13*, and *ZmE2F18* and *ZmE2F19*. Likewise, gene synteny analysis revealed one and twenty-two orthologous pairs between *ZmE2F* and *AtE2F* and *ZmE2F* and *OsE2F*, respectively (Fig. 4B; Table S3). Meanwhile, the Ka/Ks rates among *ZmE2Fs* paralogous pairs ranged from 0.19 to 0.35 and their duplication time was estimated to be 16.54–139.30 million years ago (Table S4). The results suggest that gene duplication contributed to *E2F* expansion during the evolutionary process.

Furthermore, *cis*-acting element analysis revealed that abundant stress- or hormone-responsive elements were found in the promoter regions of *ZmE2Fs*, such as ABREs, MBSs, AREs, and LTR elements (Table S5), which were responsive to abscisic acid, drought, anaerobic induction, and low temperature. For instance, ABREs were found in all *ZmE2F* promoters. MBS elements, the MYB binding site involved in drought response, were found in 15 *ZmE2F* promoters. This finding implies that the *ZmE2F* genes may be involved in abiotic stress responses.

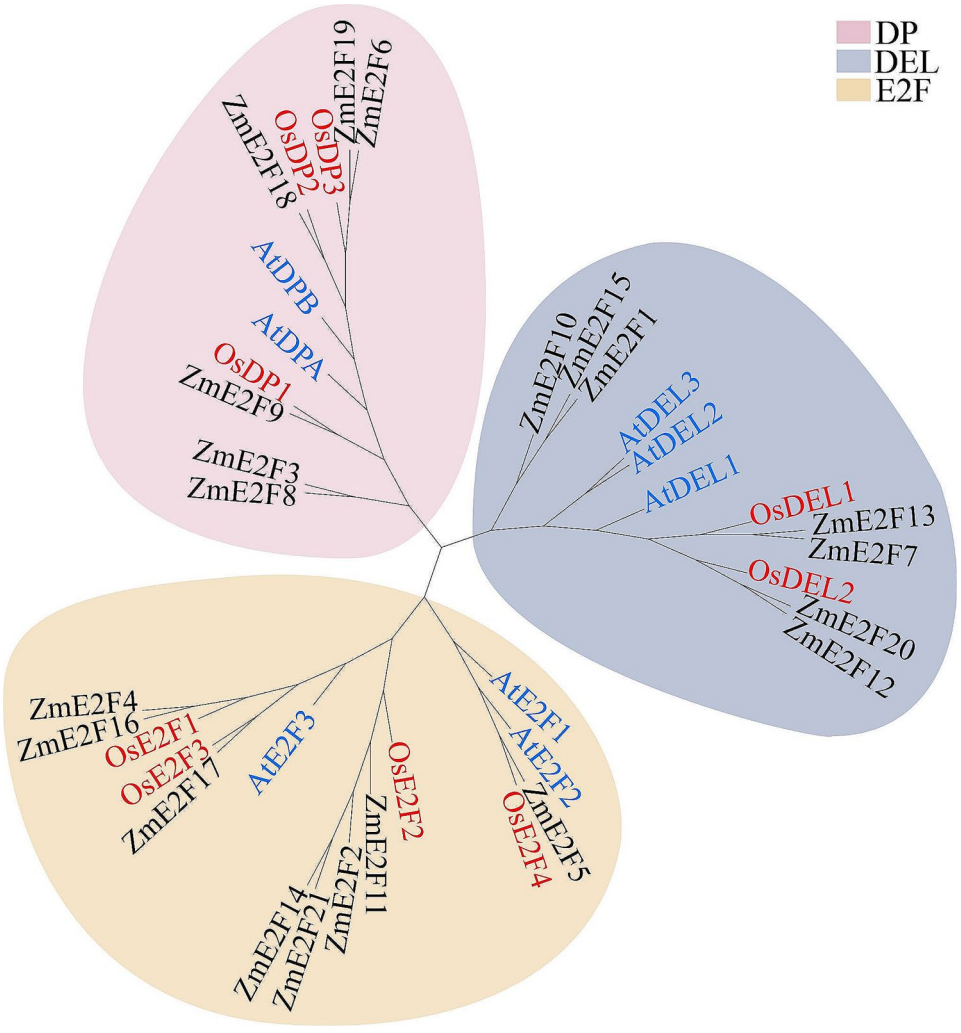

Fig. 1 Phylogenetic tree of the E2F family. The E2Fs of *Arabidopsis*, rice, and maize are marked in blue, red, and black, respectively

ZmE2F6 interacts with ZmPP2C26

In our previous study, ZmE2F6 was identified as a potential target of two ZmPP2C26 splicing variants (ZmPP2C26L/S) via Y2H library screening. Hence, to verify whether ZmE2F6 interacts with ZmPP2C26, Y2H, and GST pull-down assays were performed. As shown in Fig. 5, the yeast cells transformed with AD-*ZmE2F6* and BD-*ZmPP2C26L/S* exhibited normal growth and turned blue on SD/-Leu/-Trp/-His/-Ade plates containing X-α-gal. Moreover, the GST-ZmE2F6 protein could be pulled down by His-ZmPP2C26 L/S in the GST pull-down assay. These findings confirmed the interaction between ZmE2F6 and ZmPP2C26L/S. Likewise, there were 7 potential phosphorylated sites in ZmE2F6 amino acid sequences (Table S6) were predicted using NetPhos-3.1 (https://services.healthtech.dtu.dk/services/NetPhos-3.1/).

ZmE2F6 localized to the nucleus

To further validate the cellular localization of the ZmE2F6 protein, the ORF of *ZmE2F6* was cloned and inserted into the *35 S-eGFP* plasmid to fuse with *eGFP*. The results of transient expression in tobacco leaves revealed that fluorescent signals were observed in whole cells, including the nucleus and cytoplasm, transformed by the *35 S-eGFP* empty vector. However, in tobacco leaves transformed with *35 S-ZmE2F6-eGFP*, fluorescent signals were exclusively detected in the nucleus (Fig. 6). This observation is consistent with the bioinformatic prediction, confirming that the ZmE2F6 transcription factor is solely localized in the nucleus.

The expression of *ZmE2F6* was induced by drought stress

The qRT-PCR results demonstrated that the expression of the *ZmE2F6* gene was responsive to drought stress (Fig. 7). After drought treatment, the expression of *ZmE2F6* in maize shoots was significantly upregulated and reached approximately 11-, 8-, 100-, and 47-fold that

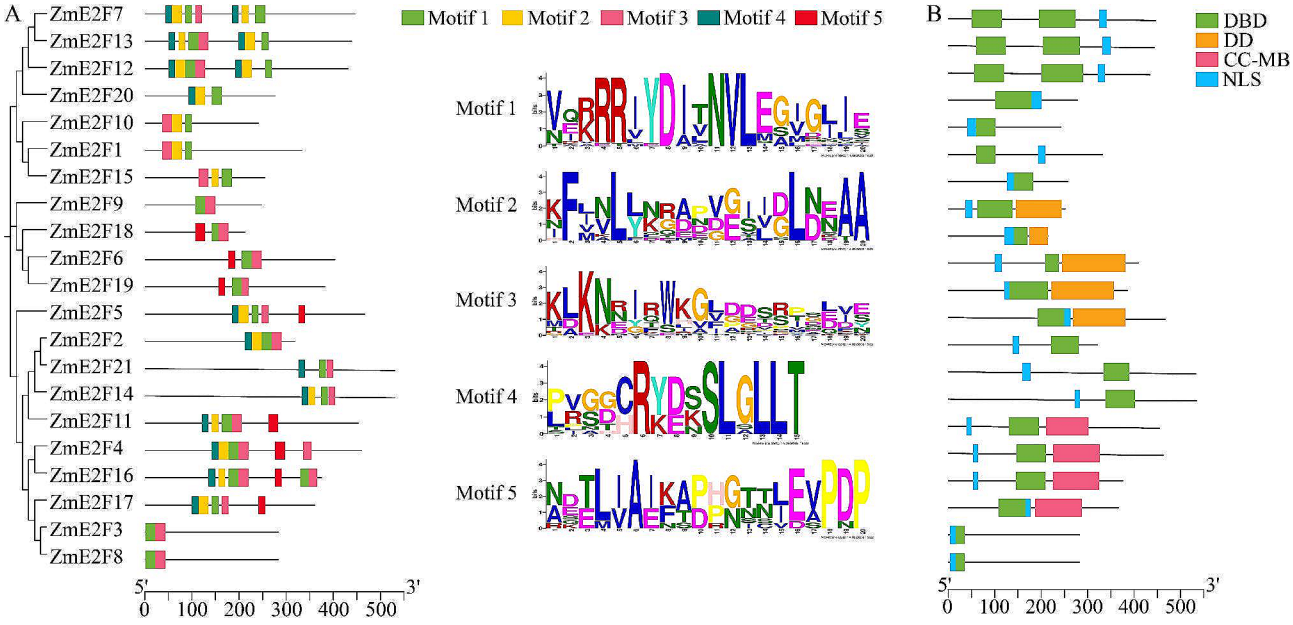

Fig. 2 Conserved motif and domain of ZmE2Fs

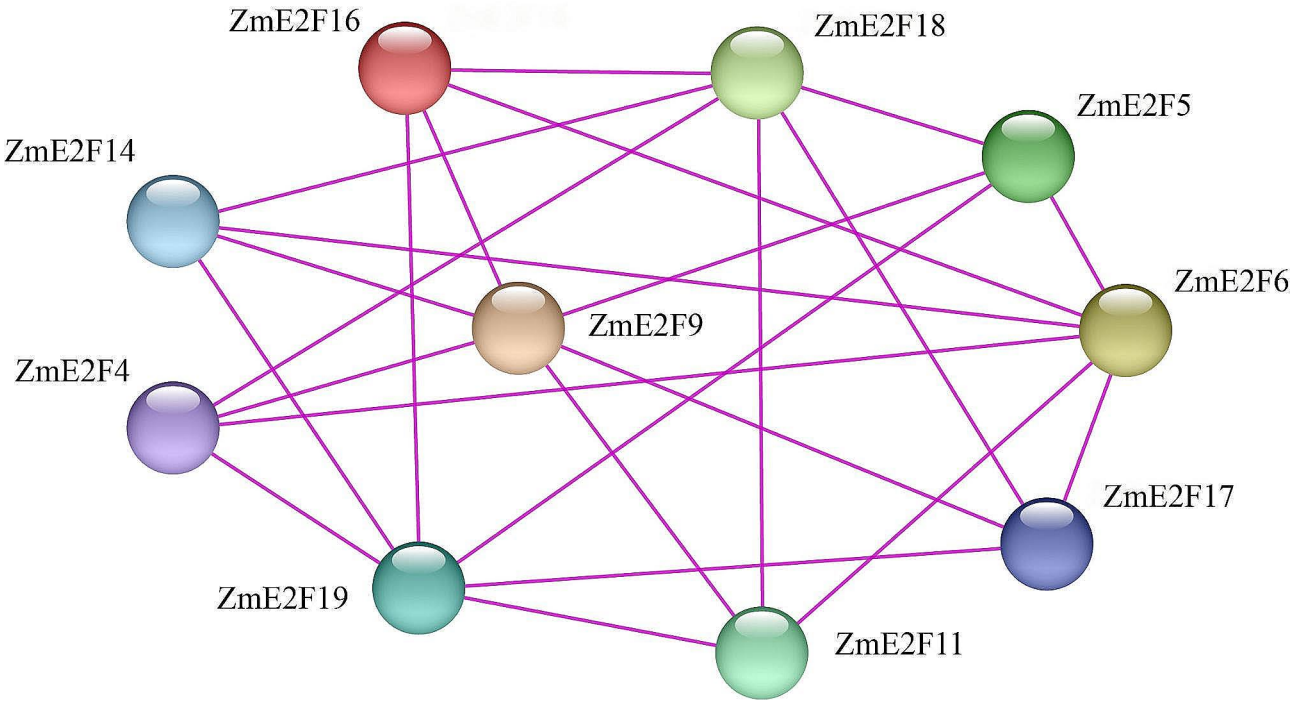

Fig. 3 ZmE2F protein-protein interaction prediction

of the control at 3, 6, 12, and 24 h of treatment. In roots, the expression of *ZmE2F6* was significantly upregulated after 3 h of drought treatment and then downregulated at 6, 12, and 24 h of treatment. These results suggest that *ZmE2F6* responds to drought stress.

Expression of *ZmE2F6* enhanced drought tolerance in *Arabidopsis thaliana*

To assess the function of ZmE2F6 in regulating drought tolerance, we generated transgenic *Arabidopsis* lines overexpressing *ZmE2F6*. In the T_1 generation, ten positive transgenic lines were screened by kanamycin on 1/2 MS plates, identified by PCR, and harvested to produce the next generation. Finally, in the T_3 generation, two

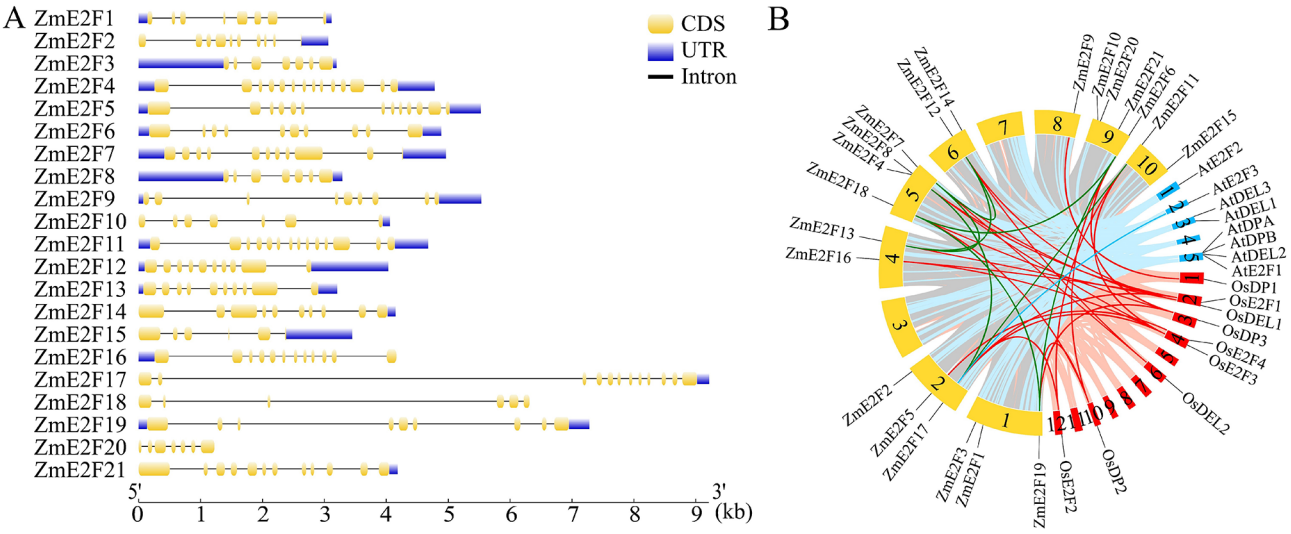

Fig. 4 Gene structure (**A**) and duplication (**B**) of ZmE2Fs. Yellow and blue boxes represent exons and untranslated regions, respectively. Black lines represent introns. Yellow, blue, and red boxes with a number represent chromosomes of maize, *Arabidopsis*, and rice, respectively. The green, blue, and red lines indicate duplicated *E2F* gene pairs among maize, as well as between maize and *Arabidopsis* and rice, respectively

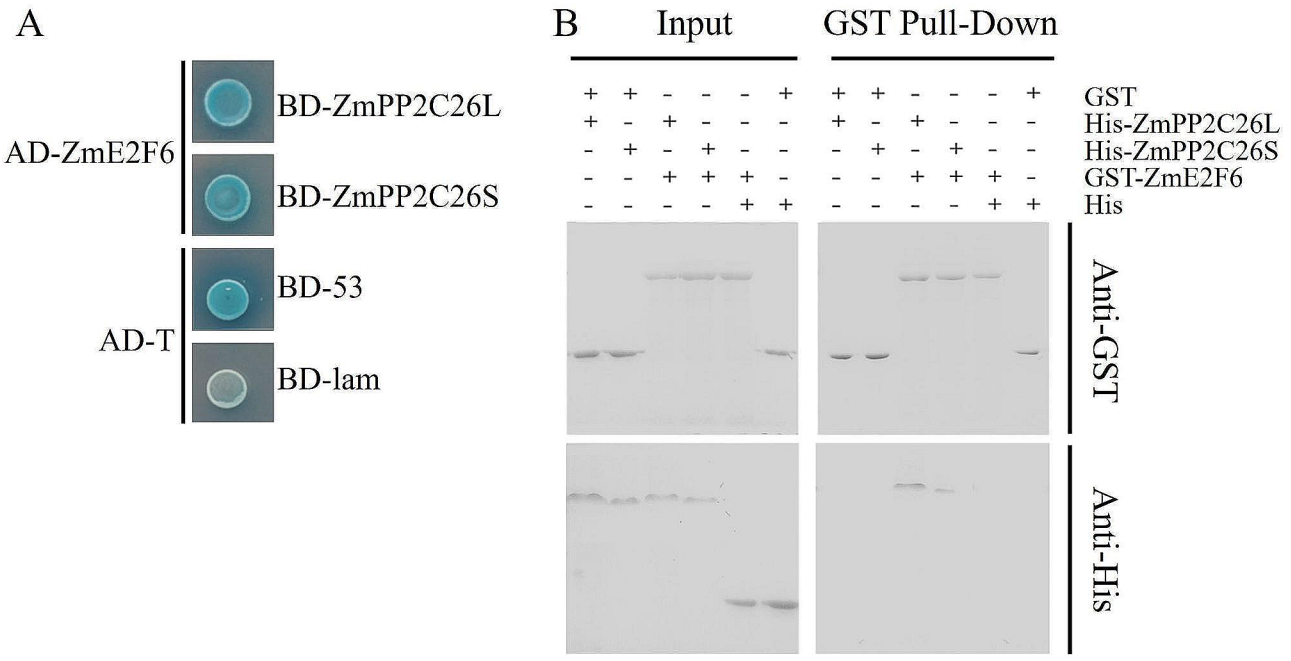

Fig. 5 ZmE2F6 interacts with ZmPP2C26. (**A**) Yeast two-hybrid (Y2H). (**B**) GST pull-down. ZmPP2C26L and ZmPP2C26S represent two splicing variants of ZmPP2C26. The combination of AD-T with BD-53 and AD-T with BD-lam were used as negative and positive controls, respectively

homozygous lines (OE6-5 and OE6-10) were selected, identified by GUS staining, and used for phenotyping (Fig. 8A). It was found that the root length of the OE6-5 and OE6-10 lines was significantly longer than that of the WT under 1/2 MS plates or supplemented with 150 mM mannitol (Fig. 8B, C). Furthermore, natural drought treatment in soil was performed to monitor the drought tolerance of the OE6-5 and OE6-10 lines. The results showed that there was no difference between the transgenic lines and WT before treatment. Subsequently, after two weeks of drought treatment, WT plants were seriously wilting, but OE6-5 and OE6-10 showed slightly inhibited phenotypes. After 3 days of rewatering, the OE-65 and OE6-10 lines exhibited significantly higher survival rates and biomass, indicating that overexpression of *ZmE2F6* contributes to enhancing drought tolerance in transgenic *Arabidopsis* and that *ZmE2F6* positively regulates drought tolerance.

To investigate the impact of ZmE2F6 overexpression on endogenous genes in *Arabidopsis thaliana*, RNA-Seq

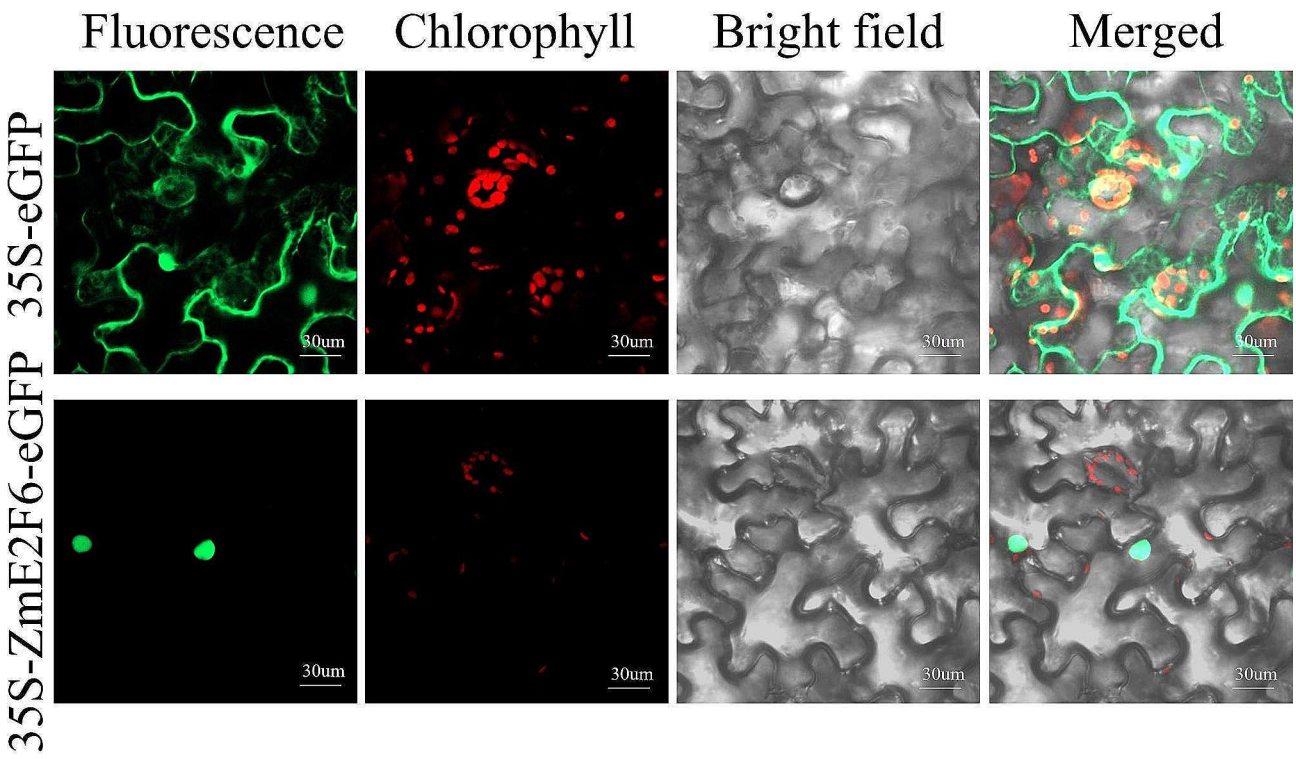

Fig. 6 Subcellular localization of ZmE2Fs

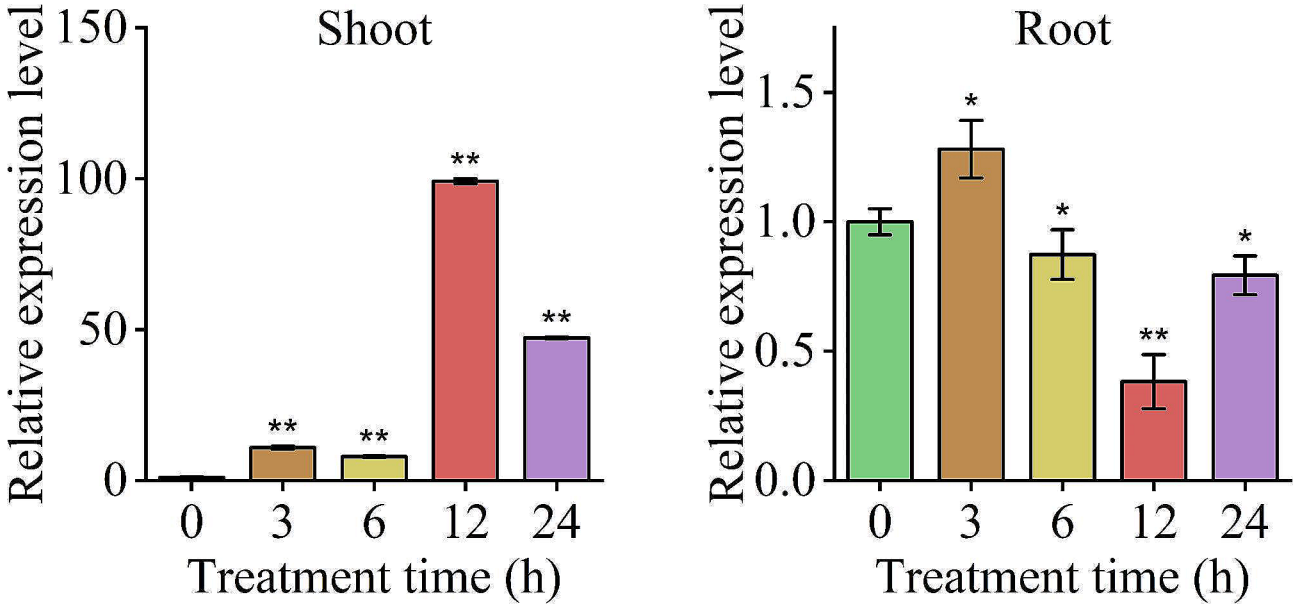

Fig. 7 The relative expression level of the *ZmE2F* gene under drought stress

was conducted on four transgenic lines, OE6-5, OE6-10, and WT. The results showed that there were 657 DEGs in transgenic lines compared to WT. Totally, 19 DEGs were identified in two transgenic lines. Among them, 15 DEGs were upregulated in transgenic lines, including *AtMYB44* (AT5G67300), *AtB1L* (AT1G18740), *AtJAZ7* (AT2G34600), *AtEXS* (AT1G35350), *AtIP5PII* (AT4G18010), *AtPATL2* (AT1G22530), *AtAZI1* (AT4G12470), *AtXTH23* (AT4G25810), and *AtEXL5* (AT2G17230) (Fig. 9). GO analysis showed that these DEGs were associated with stress responses (Figure S1).

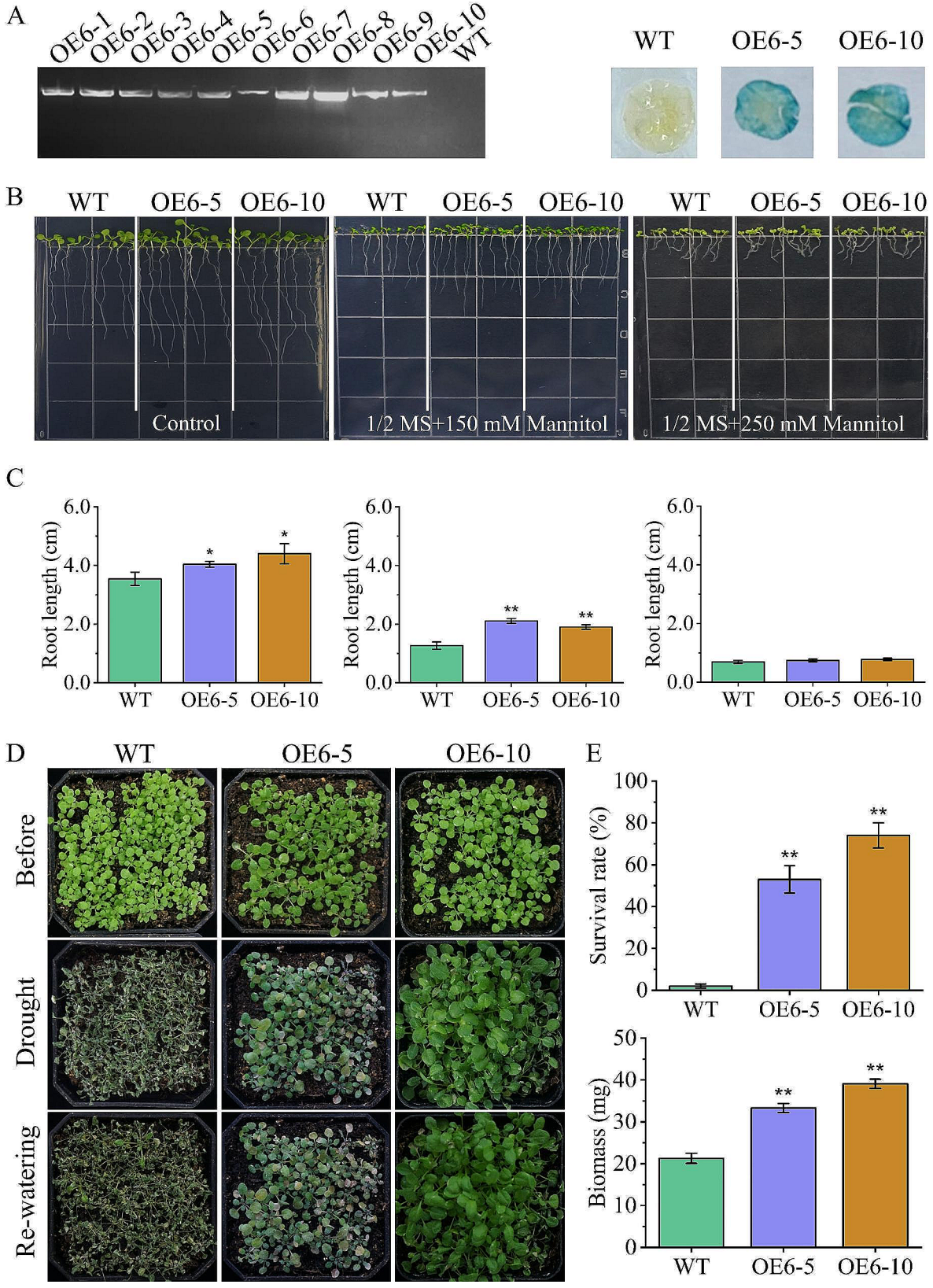

Fig. 8 The phenotype of transgenic *Arabidopsis* under drought stress. (**A**) PCR detection and GUS staining of transgenic lines. (**B**) The phenotype of transgenic lines on 1/2 MS plates with mannitol. (**C**) Root length. (**D**) The phenotype of transgenic lines in soil. (**E**) Survival rate and biomass of each line. OE6-1 to OE6-10 represent transgenic lines overexpressing *ZmE2F6*. WT, wild type

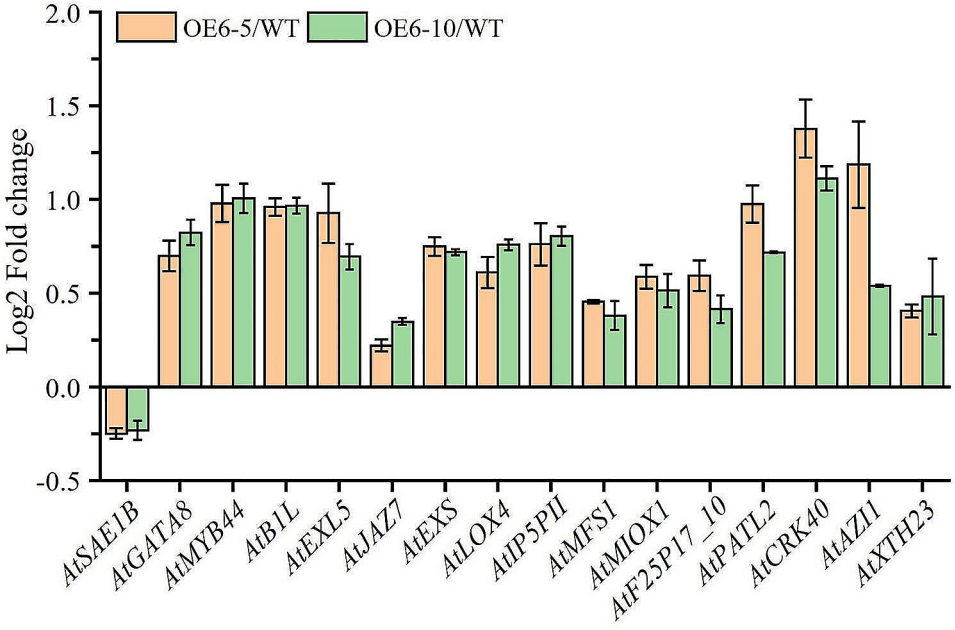

Fig. 9 The expression level (Log2 Fold change) of differentially expressed genes (DEGs) in each line

Discussion

In eukaryotes, the ZmE2F family is characterized as a TF that plays crucial roles in cell division, DNA repair, and differentiation [11, 13–16]. However, the E2F family is only genome-wide identified in a few plants, including *Arabidopsis*, rice, wheat, Moso bamboo, *Medicago truncatula*, and *Phaseolus vulgaris* [9, 24–26]. In the present study, 21 *ZmE2F* members were identified in the maize genome (Table 1) and classified into E2F, DP, and DEL subclades (Fig. 1), which was higher than the number of E2F members identified in *Arabidopsis* (8), rice (9), *Medicago truncatula* (5), and *Phaseolus vulgaris* (7) but close to the number in wheat (27) and *Moso bamboo* (23), owing to their comparable genome size and gene duplication being a major driving force of gene families [25, 49]. Likewise, eight paralogous pairs of *ZmE2Fs* and twenty-three orthologous pairs of *E2Fs* among maize, *Arabidopsis*, and rice were found (Fig. 4). All the Ka/Ks ratios of the ZmE2Fs paralogous pairs were <1 (Table S4), indicating their duplication evolved under purifying selection [50]. A similar phenomenon was consistently observed in the *PheE2F/DP* gene family [25]. A previous study showed that there are 12 *ZmE2F* genes in maize [51], which is much lower than the number identified in this study. This may be due to their preliminary BLAST search using maize genome release 5b.60 and not a comprehensive analysis [51].

All ZmE2F proteins possess at least one DBD characterized by motif 1 containing the RRIYD sequence and dimerization residue DNVLE sequence (Fig. 2), which contributes to the binding of E2F and DNA as a homodimer or as a heterodimer with its dimerization partner DP. In addition, some ZmE2F proteins also have DD and CC-MB domains, which promotes their formation of heterodimers to regulate downstream genes [52]. As a result, ten ZmE2Fs are predicted to interact with each other and generate 23 PPI combinations (Fig. 3), owing to the presence of the DNVLE residues, DD, or CC-MB domain in these proteins.

To date, the function of E2F in regulating plant stress tolerance remains unknown, although few reports have shown that the expression of some *E2F* genes is responsive to stress [9, 24–26]. In our study, abundant stress-responsive acting elements were found in *ZmE2F* promoter regions, such as ABREs and MBSs, suggesting the response of *ZmE2Fs* to stress and the potential roles of *ZmE2Fs*. In our previous study, the *ZmPP2C26* gene, a B clade of maize *PP2C* members, was found to be responsive to drought stress and negatively regulated drought tolerance in *Arabidopsis*, rice, and maize [36] and targeted on maize *ZmE2F6* (Zm00001d048412), indicating its function in the drought response. Hence, the *ZmE2F6* gene was cloned and functionally validated. It is found that the ZmE2F6 interacts with two splicing variants of ZmPP2C26 but localized in the nucleus (Figs. 5 and 6), suggesting that ZmPP2C26 physically targets ZmE2F6. In *Arabidopsis*, it has been previously reported that B clade PP2C (AP2C1) dephosphorylates the autophosphorylated form of CBL-interacting protein kinase 9 (CIPK9) to regulate root growth, seedling development, and stress tolerance (low-K^+) [53]. Previous studies showed that BES1/BZR1 TFs are phosphorylated and degraded but moved to the nucleus after dephosphorylation in the cytoplasm [54, 55]. It is proposed that ZmPP2C26 might

dephosphorylate ZmE2F6 in the cytoplasm, which needs to be further revealed in our next study.

The qRT-PCR results showed that the *ZmE2F6* gene was induced by drought stress (Fig. 7), which could be explained by the presence of three MBS and two ABREs in the *ZmE2F6* promoter (Table S5). It's confirmed that MYB transcription factors bind to the MYB binding sites (MBS) of nuclear gene promoters to adjust their transcription and regulate drought tolerance in plants [56, 57]. Likewise, ABRE (ABA-responsive element), the major *cis*-element for ABA-responsive gene expression, is targeted by ABRE-binding protein (AREB) or ABRE-binding factor (ABF) TFs to regulate the drought response via the ABA signaling pathway [58]. These findings further imply the regulation of *ZmE2F6* in drought tolerance.

After overexpressing *ZmE2F6* in *Arabidopsis*, the transgenic lines showed longer root lengths than the WT (Fig. 8B, C), which is consistent with the fact that E2Fs regulate root growth in *Arabidopsis* [19, 22, 59]. The elevated root growth of *ZmE2F6*-overexpressing lines may confer osmotic tolerance because roots can respond to moisture and coordinate responses to drought [1]. The ectopic expression of *ZmE2F6* enhances drought tolerance in transgenic *Arabidopsis* (Fig. 8). We found that some stress-related genes were significantly upregulated in the transgenic lines, such as *AtMYB44*, *AtB1L*, *AtJAZ7*, *AtEXS*, *AtIP5PII*, *AtPATL2*, *AtAZI1*, *AtXTH23*, and *AtEXL5* (Fig. 9), which are well known to regulate abiotic stresses [60–68]. The ZmE2F6 protein acts as a TF and localizes in the nucleus to regulate the expression of these genes (Fig. 6). However, the molecular mechanism regulated by ZmE2F6 in maize remains unknown.

Conclusion

Overall, in this study, a comprehensive analysis of the *ZmE2F* gene family was performed. In total, 21 ZmE2F TFs were identified in the maize genome and divided into three subclades. All ZmE2F proteins possessed at least one DBD characterized by the RRIYD (DNA binding motif) and DNVLE (dimerization residues) sequences. The *ZmE2F* genes showed diversity in gene structure, expanded by gene duplication, and contained abundant stress-responsive elements in their promoter regions. Then, the *ZmE2F6* gene was cloned and functionally verified in the drought response. The ZmE2F6 protein interacted with ZmPP2C26, localized in the nucleus, and responded to drought treatment. The overexpression of *ZmE2F6* enhanced drought tolerance in transgenic *Arabidopsis* by upregulating stress-related gene transcription. This study sheds light on the role of ZmE2F in the drought response and provides novel insights into a greater understanding of the E2F family in crops.

Supplementary Information

The online version contains supplementary material available at https://doi.org/10.1186/s12864-024-10369-0.

Supplementary Material 1

Supplementary Material 2

Acknowledgements
Not applicable.

Author contributions
Y.C., K.W. and F.L. designed and carried out the experiments; Y.C., K.W., B.L., H.M. and Y.W. carried out all bioinformatics analysis and wrote the manuscript; Q. Y. provided technical support. F.F., W.L. and H.Y supervised the experiments; H.Y. directed and revised the manuscript. All authors reviewed and approved the final manuscript.

Funding
This study was supported by the National Key R&D Program of China (2021YFF1000303), the Sichuan Science and Technology Program (2022YFH0067) and the National Natural Science Foundation of China (32102226).

Data availability
The RNA-seq datasets generated during the current study are available in the NCBI repository under BioProject accession number PRJNA1028664.

Declarations

Ethics approval and consent to participate
Not applicable.

Consent for publication
Not applicable.

Competing interests
The authors declare no competing interests.

Received: 10 October 2023 / Accepted: 2 May 2024
Published online: 13 May 2024

References

1. Gupta A, Rico-Medina A, Caño-Delgado AI. The physiology of plant responses to drought. Science. 2020;368:266–9.
2. Zhang H, Zhu J, Gong Z, Zhu J. Abiotic stress responses in plants. Nat Rev Genet. 2022;23:104–19.
3. Zhu JK. Abiotic stress signaling and responses in plants. Cell. 2016;167:313–24.
4. Hrmova M, Hussain SS. Plant transcription factors involved in drought and associated stresses. Int J Mol Sci. 2021;22:5662.
5. Manna M, Thakur T, Chirom O, Mandlik R, Deshmukh R, Salvi P. Transcription factors as key molecular target to strengthen the drought stress tolerance in plants. Physiol Plant. 2021;172:847–68.
6. Saharan BS, Brar B, Duhan JS, Kumar R, Marwaha S, Rajput VD, et al. Molecular and physiological mechanisms to mitigate abiotic stress conditions in plants. Life (Basel). 2022;12:1634.
7. Nevins JR. E2F: a link between the rb tumor suppressor protein and viral oncoproteins. Science. 1992;258:424–9.
8. Van Den Heuvel S, Dyson NJ. Conserved functions of the pRB and E2F families. Nat Rev Mol Cell Biol. 2008;9:713–24.
9. Ma TY, Li ZW, Zhang SY, Liang GT, Guo J. Identification and expression analysis of the E2F/DP genes under salt stress in *Medicago truncatula*. Genes Genomics. 2014;36:819–28.
10. Vandepoele K, Raes J, De Veylder L, Rouzé P, Rombauts S, Inzé D. Genome-wide analysis of core cell cycle genes in *Arabidopsis*. Plant Cell. 2002;14:903–16.

11. Gómez MS, Sheridan ML, Casati P. E2Fb and E2Fa transcription factors independently regulate the DNA damage response after ultraviolet B exposure in *Arabidopsis*. Plant J. 2022;109:1098–115.
12. Liu Y, Lai J, Yu M, Wang F, Zhang J, Jiang J, et al. The *Arabidopsis* SUMO E3 ligase AtMMS21 dissociates the E2Fa/DPa complex in cell cycle regulation. Plant Cell. 2016;28:2225–37.
13. Manickavinayaham S, Dennehey BK, Johnson DG. Direct regulation of DNA repair by E2F and RB in mammals and plants: core function or convergent evolution? Cancers (Basel). 2021;13:1–14.
14. Perrotta L, Giordo R, Francis D, Rogers HJ, Albani D. Molecular analysis of the E2F/DP gene family of daucus carota and involvement of the DcE2F1 factor in cell proliferation. Front Plant Sci. 2021;12:652570.
15. Wang L, Chen H, Wang C, Hu Z, Yan S. Negative regulator of E2F transcription factors links cell cycle checkpoint and DNA damage repair. Proc Natl Acad Sci U S A. 2018;115:E3837–45.
16. Yuan R, Liu Q, Segeren HA, Yuniati L, Guardavaccaro D, Lebbink RJ, et al. Cyclin F-dependent degradation of E2F7 is critical for DNA repair and G2-phase progression. EMBO J. 2019;38:e101430.
17. Del Pozo JC, Boniotti MB, Gutierrez C. Arabidopsis E2Fc functions in cell division and is degraded by the ubiquitin-SCFAtSKP2 pathway in response to light. Plant Cell. 2002;14:3057–71.
18. Del Pozo JC, Diaz-Trivino S, Cisneros N, Gutierrez C. The balance between cell division and endoreplication depends on E2FC-DPB, transcription factors regulated by the ubiquitin-SCFSKP2A pathway in *Arabidopsis*. Plant Cell. 2006;18:2224–35.
19. Sozzani R, Maggio C, Varotto S, Canova S, Bergounioux C, Albani D, et al. Interplay between *Arabidopsis* activating factors E2Fb and E2Fa in cell cycle progression and development. Plant Physiol. 2006;140:1355–66.
20. De Veylder L, Beeckman T, Beemster GTS, De Almeida Engler J, Ormenese S, Maes S, et al. Control of proliferation, endoreduplication and differentiation by the *Arabidopsis* E2Fa-DPa transcription factor. EMBO J. 2002;21:1360–8.
21. Chandran D, Rickert J, Huang Y, Steinwand MA, Marr SK, Wildermuth MC. Atypical E2F transcriptional repressor DEL1 acts at the intersection of plant growth and immunity by controlling the hormone salicylic acid. Cell Host Microbe. 2014;15:506–13.
22. Nakagami S, Saeki K, Toda K, Ishida T, Sawa S. The atypical E2F transcription factor DEL1 modulates growth-defense tradeoffs of host plants during root-knot nematode infection. Sci Rep. 2020;10:8836.
23. Guo XY, Wang Y, Zhao PX, Xu P, Yu GH, Zhang LY, et al. AtEDT1/HDG11 regulates stomatal density and water-use efficiency via ERECTA and E2Fa. New Phytol. 2019;223:1478–88.
24. Zhang H, Jiang W, Xia P, Yin J, Chen H, Li W, et al. Genome-wide identification transcriptional expression analysis of E2F-DP transcription factor family in wheat. Plant Mol Biol Rep. 2022;40:339–58.
25. Li L, Shi Q, Li Z, Gao J. Genome-wide identification and functional characterization of the PheE2F/DP gene family in *Moso bamboo*. BMC Plant Biol. 2021;21:1–15.
26. Okay A, Amirinia K, Buyuk I. E2F/DP protein family in beans: identification, evolution and expression analysis within the genome. South Afr J Bot. 2023;157:122–34.
27. Singh A, Pandey H, Pandey S, Lal D, Chauhan D, Aparna, Antre SH, Kumar BS. Drought stress in maize: stress perception to molecular response and strategies for its improvement. Funct Integr Genomics. 2023;23:296.
28. Lobell DB, Deines JM, Tommaso S, Di. Changes in the drought sensitivity of US maize yields. Nat Food. 2020;1:729–35.
29. Simpkins G. Maize sensitivity to drought. Nat Rev Earth Environ. 2020;1:625–625.
30. Yang Z, Cao Y, Shi Y, Qin F, Jiang C, Yang S. Genetic and molecular exploration of maize environmental stress resilience: toward sustainable agriculture. Mol Plant. 2023;16:1–22.
31. Liu B, Zhang B, Yang Z, Liu Y, Yang S, Shi Y, et al. Manipulating ZmEXPA4 expression ameliorates the drought-induced prolonged anthesis and silking interval in maize. Plant Cell. 2021;33:2058–71.
32. Nuccio ML, Wu J, Mowers R, Zhou HP, Meghji M, Primavesi LF, et al. Expression of trehalose-6-phosphate phosphatase in maize ears improves yield in well-watered and drought conditions. Nat Biotechnol. 2015;33:862–9.
33. Tian T, Wang S, Yang S, Yang Z, Liu S, Wang Y, et al. Genome assembly and genetic dissection of a prominent drought-resistant maize germplasm. Nat Genet. 2023;55:496–506.
34. Xiang Y, Sun X, Bian X, Wei T, Han T, Yan J, et al. The transcription factor ZmNAC49 reduces stomatal density and improves drought tolerance in maize. J Exp Bot. 2021;72:1399–410.
35. Singh A, Pandey H, Pandey S, Lal D, Chauhan D, Aparna, et al. Drought stress in maize: stress perception to molecular response and strategies for its improvement. Funct Integr Genomics. 2023;23:1–19.
36. Lu F, Li W, Peng Y, Cao Y, Qu J, Sun F, et al. ZmPP2C26 alternative splicing variants negatively regulate drought tolerance in maize. Front Plant Sci. 2022;13:1–13.
37. Chen C, Chen H, Zhang Y, Thomas HR, Frank MH, He Y, et al. TBtools: an integrative toolkit developed for interactive analyses of big biological data. Mol Plant. 2020;13:1194–202.
38. Szklarczyk D, Gable AL, Lyon D, Junge A, Wyder S, Huerta-Cepas J, et al. STRING v11: protein-protein association networks with increased coverage, supporting functional discovery in genome-wide experimental datasets. Nucleic Acids Res. 2019;47:D607–13.
39. Gaut BS, Morton BR, Mccaig BC, Clegg MT. Substitution rate comparisons between grasses and palms: synonymous rate differences at the nuclear gene adh parallel rate differences at the plastid gene rbcL. Proc Natl Acad Sci. 1996;93:10274–9.
40. Sun F, Yu H, Qu J, Cao Y, Ding L, Feng W, et al. Maize ZmBES1/BZR1-5 decreases ABA sensitivity and confers tolerance to osmotic stress in transgenic *Arabidopsis*. Int J Mol Sci. 2020;21:996.
41. Livak KJ, Schmittgen TD. Analysis of relative gene expression data using real-time quantitative PCR and the $2^{-\Delta\Delta Ct}$ method. Methods. 2001;25:402–8.
42. Clough SJ, Bent AF. Floral dip: a simplified method for *Agrobacterium*-mediated transformation of *Arabidopsis thaliana*. Plant J. 1998;16:735–43.
43. Kim D, Langmead B, Salzberg SL. HISAT: A fast spliced aligner with low memory requirements. Nat Methods. 2015;12:357–60.
44. Pertea M, Kim D, Pertea GM, Leek JT, Salzberg SL. Transcript-level expression analysis of RNA-seq experiments with HISAT, StringTie and Ballgown. Nat Protoc. 2016;11:1650–67.
45. Love MI, Huber W, Anders S. Moderated estimation of Fold change and dispersion for RNA-seq data with DESeq2. Genome Biol. 2014;15:1–21.
46. Xie C, Mao X, Huang J, Ding Y, Wu J, Dong S, et al. KOBAS 2.0: a web server for annotation and identification of enriched pathways and diseases. Nucleic Acids Res. 2011;39:W316–22.
47. Guo J, Song J, Wang F, Zhang XS. Genome-wide identification and expression analysis of rice cell cycle genes. Plant Mol Biol. 2007;64:349–60.
48. Lammens T, Li J, Leone G, De Veylder L. Atypical E2Fs: new players in the E2F transcription factor family. Trends Cell Biol. 2009;19:111–8.
49. Edger PP, Pires JC. Gene and genome duplications: the impact of dosage-sensitivity on the fate of nuclear genes. Chromosom Res. 2009;17:699–717.
50. Kondrashov F, Rogozin I, Wolf Y, Koonin E. Selection in the evolution of gene duplications. Genome Biol. 2002;3:RESEARCH0008.
51. Sánchez-Camargo VA, Suárez-Espinoza C, Romero-Rodríguez S, Garza-Aguilar SM, Stam M, García-Ramírez E, et al. Maize E2F transcription factors. Expression, association to promoters of S-phase genes and interaction with the RBR1 protein in chromatin during seed germination. Plant Sci. 2020;296:110491.
52. Rubin SM, Gall AL, Zheng N, Pavletich NP. Structure of the rb C-terminal domain bound to E2F1-DP1: a mechanism for phosphorylation-induced E2F release. Cell. 2005;123:1093–106.
53. Singh A, Yadav AK, Kaur K, Sanyal SK, Jha SK, Fernandes JL, et al. A protein phosphatase 2 C, AP2C1, interacts with and negatively regulates the function of CIPK9 under potassium-deficient conditions in *Arabidopsis*. J Exp Bot. 2018;69:4003–15.
54. He G, Liu J, Dong H, Sun J. The Blue-Light receptor CRY1 interacts with BZR1 and BIN2 to modulate the phosphorylation and nuclear function of BZR1 in repressing BR signaling in *Arabidopsis*. Mol Plant. 2019;12:689–703.
55. Khan TA, Kappachery S, Karumannil S, AlHosani M, Almansoori N, Almansoori H, et al. Brassinosteroid signaling pathways: insights into plant responses under abiotic stress. Int J Mol Sci. 2023;24:17246.
56. Prouse MB, Campbell MM. The interaction between MYB proteins and their target DNA binding sites. Biochim Biophys Acta. 2012;1819:67–77.
57. Wang X, Niu Y, Zheng Y. Multiple functions of MYB transcription factors in abiotic stress responses. Int J Mol Sci. 2021;22:6125.
58. Nakashima K, Yamaguchi-Shinozaki K. ABA signaling in stress-response and seed development. Plant Cell Rep. 2013;32:959–70.
59. He SS, Liu J, Xie Z, O'Neill D, Dotson S. *Arabidopsis* E2Fa plays a bimodal role in regulating cell division and cell growth. Plant Mol Biol. 2004;56:171–84.
60. Jaradat MR, Feurtado JA, Huang D, Lu Y, Cutler AJ. Multiple roles of the transcription factor AtMYBR1/AtMYB44 in ABA signaling, stress responses, and leaf senescence. BMC Plant Biol. 2013;13:192.

61. Chen T, Zhang W, Yang G, Chen JH, Chen BX, Sun R, et al. TRANSTHYRETIN-LIKE and BYPASS1-LIKE co-regulate growth and cold tolerance in *Arabidopsis*. BMC Plant Biol. 2020;20:332.
62. Tellström V, Usadel B, Thimm O, Stitt M, Küster H, Niehaus K. The lipopolysaccharide of Sinorhizobium meliloti suppresses defense-associated gene expression in cell cultures of the host plant *Medicago truncatula*. Plant Physiol. 2007;143:825–37.
63. Meng L, Zhang T, Geng S, Scott PB, Li H, Chen S. Comparative proteomics and metabolomics of JAZ7-mediated drought tolerance in *Arabidopsis*. J Proteom. 2019;196:81–91.
64. Maathuis FJM, Filatov V, Herzyk P, Krijger GC, Axelsen KB, Chen S, et al. Transcriptome analysis of root transporters reveals participation of multiple gene families in the response to cation stress. Plant J. 2003;35:675–92.
65. Kaye Y, Golani Y, Singer Y, Leshem Y, Cohen G, Ercetin M, et al. Inositol polyphosphate 5-phosphatase7 regulates the production of reactive oxygen species and salt tolerance in *Arabidopsis*. Plant Physiol. 2011;157:229–41.
66. Wege S, Ugalde JM. Metal health: PATELLIN2 reduces iron-induced toxicity in *Arabidopsis*. Plant Physiol. 2023;192:15–6.
67. Atkinson NJ, Lilley CJ, Urwin PE. Identification of genes involved in the response of *Arabidopsis* to simultaneous biotic and abiotic stresses. Plant Physiol. 2013;162:2028–41.
68. Xu P, Fang S, Chen H, Cai W. The brassinosteroid-responsive xyloglucan endotransglucosylase/hydrolase 19 (XTH19) and XTH23 genes are involved in lateral root development under salt stress in *Arabidopsis*. Plant J. 2020;104:59–75.

Publisher's Note